https://doi.org/10.5194/egusphere-2026-4869
Preprint. Discussion started: 21 August 2026

Coral reef–influenced air masses promote new particle formation over the Great Barrier Reef

Magdalena Okuljar[1]*, Juha Sulo[1]*†, Joel Alroe[1], Zijun Li[1], Branka Miljevic[1], Daniel Harrison[2], Zoran Ristovski[1]

[1] School of Earth and Atmospheric Sciences, Queensland University of Technology, Brisbane, Australia

[2]Reefs and Oceans Research Cluster, National Marine Science Centre, Southern Cross University, Coffs Harbour, NSW, Australia

* The first and second author contributed equally to this work

[†]Now at Institute of Atmospheric and Earth System Science/Physics, University of Helsinki, 00014, Helsinki, Finland

Correspondence to: Magdalena Okuljar (magdalena.okuljar@qut.edu.au) and Zoran Ristovski (z.ristovski@qut.edu.au)

Abstract

Coral reefs are among the most biologically important ecosystems on Earth and are highly sensitive to climate change. The Great Barrier Reef (GBR) is the largest coral reef system globally, yet the extent to which it contributes to local atmospheric particle loading remains poorly understood. Here, we present a case study focusing on particle formation processes observed during a six-week measurement campaign at Heron Island on the GBR. Our results show that when air masses spent considerable time over the reef itself, we observed a number of new particle formation events. These events were preceded by an increase in dimethylsulfoxide (DMSO) concentrations and led to increased sulfate and ammonium in the resulting particle population. Importantly, DMSO concentrations were not higher during event days in comparison to other days, suggesting that both precursor availability and favorable photochemical conditions such as increased solar irradiance played a role in initiating particle formation over the reef. These findings provide evidence that the GBR ecosystem can influence local aerosol formation processes, with implications for regional cloud formation and climate feedbacks in marine ecosystems.

1. Introduction

The Great Barrier Reef (GBR) is the largest reef ecosystem in the world and an important economical, natural and cultural heritage site (Harris et al., 2018; Knowlton et al., 2010; Reaka, 1997; Rowland et al., 2025; Santavy et al., 2021). However, the GBR as well as other coral reefs around the world are under significant stress from increased ocean temperatures, ocean acidification, extreme weather events and habitat destruction (Dietzel et al., 2021; Fox-Kemper et al., 2021; Hughes et al., 2017b, a). The GBR has also seen an increased number of coral bleaching events, with severe bleaching an almost annual phenomenon in the 2020s (AIMS, 2025; Hughes et al., 2018). Due to this, the Reef

https://doi.org/10.5194/egusphere-2026-4869
Preprint. Discussion started: 21 August 2026

Restoration and Adaptation Program (RRAP) focuses on developing strategies to help the GBR resist and adapt to the impacts of climate change (Anthony et al., 2020; Condie et al., 2021).

The RRAP Cooling and Shading subprogram focused on developing methods to cool and shade the reef. Some of the more promising interventions involved the introduction of additional aerosol particles into the atmosphere to increase the refraction of solar radiation away from the reef (Bay et al., 2019; Braga et al., 2025; Harrison, 2024; Hernandez-Jaramillo et al., 2024; Khan et al., 2025; Li et al., 2025). Aerosol particles play a key role in the Earth's climate system through their interactions with radiation and clouds (Storelvmo et al., 2016). Aerosol particles can act as cloud condensation nuclei (CCN), influencing cloud droplet number concentrations, cloud albedo, and precipitation processes (Albrecht, 1989; Twomey, 1974). The properties of these particles, including their size distribution, chemical composition, and hygroscopicity, are strongly influenced by both atmospheric transport and local sources of precursor gases (Dusek et al., 2006; Petters and Kreidenweis, 2007). In relatively clean marine environments where aerosol particle number concentrations are well below 1000 cm^{-3}, such as the GBR region (Braga et al., 2025; Eckert et al., 2024; Hernandez-Jaramillo et al., 2024; Horchler et al., 2025; Sulo et al., 2026a), small changes in aerosol precursor availability or atmospheric oxidation conditions can have disproportionate effects on particle formation processes and CCN populations (Kerminen et al., 2018; Quinn and Bates, 2011). Accurate representation of these relationships in regional models is challenging and requires adequate validation through measurement studies. However, due to its remote location, aerosol dynamics over the GBR have been mostly studied by satellite measurements and modelling (Cropp et al., 2018; Fiddes et al., 2022; Jackson et al., 2018; Swan, 2022).

Coral reef environments are known to emit a variety of aerosol precursors that can influence atmospheric chemistry and aerosol formation (Broadgate et al., 1997). In particular, marine ecosystems produce S-containing compounds such as dimethyl sulfide (DMS), which is generated by phytoplankton, algae, and coral-associated symbiotic organisms (Deschaseaux et al., 2015; Stefels et al., 2007). Once emitted to the atmosphere, DMS undergoes oxidation to form products including dimethyl sulfoxide (DMSO), sulfur dioxide, and ultimately sulfuric acid, which can contribute to aerosol particle formation and growth in the marine boundary layer (Berndt et al., 2023; Chen et al., 2018). These processes have been proposed as part of a climate-relevant feedback linking marine biological activity to aerosol formation and cloud properties over the ocean (Charlson et al., 1987). While the role of marine sulfur emissions in aerosol formation has been widely studied in open ocean environments, much less is known about how coral reef ecosystems influence local aerosol chemistry and particle formation (Fiddes et al., 2022; Modini et al., 2009; Swan et al., 2016).

New particle formation (NPF), a process in which molecular clusters grow into stable aerosol particles, represents an important pathway for generating atmospheric aerosol. NPF has been extensively documented in continental and forested environments, where

https://doi.org/10.5194/egusphere-2026-4869
Preprint. Discussion started: 21 August 2026

sulfuric acid, organic vapors, ammonia, and amines are known to play important roles in stabilizing molecular clusters and enabling particle growth (Kerminen et al., 2018; Lehtipalo et al., 2025). NPF has also been observed in marine and coastal environments (Peltola et al., 2022; Zheng et al., 2021). However, the occurrence and controlling mechanisms of NPF at the GBR remain poorly understood.

Despite these potential links, observational studies directly connecting coral reef emissions to aerosol formation remain limited. Previous work has suggested that while reef-derived emissions may not strongly influence regional aerosol populations at large spatial and temporal scales, they could still contribute to particle formation or growth processes at local scale or mesoscale (Fiddes et al., 2022; Sulo et al., 2026b). Characterizing these interactions requires coordinated measurements of aerosol properties, trace gases, and meteorological conditions within the reef environment.

To address these questions, we conducted an intensive six-week atmospheric measurement campaign at Heron Island, located near the southern most extent of the GBR, during late 2024. A comprehensive suite of real-time aerosol and trace gas instruments was deployed to measure particle concentration and size distributions, cloud condensation nuclei (CCN), black carbon, aerosol chemical composition, and volatile organic compounds (VOCs). These measurements provide a detailed picture of the atmospheric composition over the reef and its variability under different meteorological conditions.

In this study, we aim to (i) characterize typical aerosol and air quality conditions in the reef environment, (ii) examine how meteorology and air-mass transport influence aerosol properties, (iii) investigate the occurrence and characteristics of new particle formation events, and (iv) assess the potential contribution of reef-derived emissions to local aerosol populations. Understanding these processes is important not only for improving our knowledge of atmospheric chemistry in coral reef environments, but also for assessing how biological–atmospheric interactions may influence cloud formation and climate at local and regional scales.

2. Methods

2.1. Site Description

The field measurements took place at the University of Queensland's Heron Island Research Station (Fig. 1), located on Heron Island (-23.442728 N, +151.913440 E) in the Capricorn Group of the southern GBR, approximately 80 km off the coast of Queensland, Australia. The research station is on the south side of the island, roughly 100 meters from the shoreline. The island's environment is characteristic of a coral cay; a flat, sandy island atop a coral reef platform. Surrounding reef flats are exposed at low tide and submerged at high tide, potentially affecting local aerosol and vapor sources. The meteorological conditions in November–December are typically tropical, with warm temperatures, predominantly southeasterly trade winds, and high relative humidity (RH) typically above 70%. The main on-site sources of anthropogenic pollutants are the station's power generators, cooking emissions from gas stoves on the island and occasional boat traffic. This setting provides a

https://doi.org/10.5194/egusphere-2026-4869
Preprint. Discussion started: 21 August 2026

clean marine background punctuated by natural reef-related emissions and intermittent localized pollution resulting from human activity.

Figure 1. Map of Heron Island (© Google Maps 2025). The position of a laboratory used for atmospheric measurement is marked with a purple triangle.

2.2. Instrumentation

A broad range of instruments was deployed to measure particle-phase, gas-phase, and meteorological parameters (Table S1) during November-December 2024 (for a detailed timeline see S1). All aerosol and trace gas instruments drew air from a common sampling inlet mounted on the roof of the lab, approximately 12 m above ground level. The inlet consisted of 6 meters of 1-inch stainless steel tubing running vertically and then horizontally through a wall into the laboratory. The design included a laminar-flow inlet manifold that split the flow to feed each instrument. Aerosol size distributions were measured by a Neutral cluster and Air Ion Spectrometer (NAIS, Airel Ltd.) measuring mobility size distributions of 0.8 – 42 nm ions and ~2.5– 42 nm neutral particles, a Scanning Electrical Mobility Spectrometer (SEMS, Brechtel Inc.) measuring 10–800 nm particle size distributions, and an Aerodynamic Particle Sizer (APS, TSI Inc.) for particles 0.5–20 µm. These three instruments together provided the aerosol size distribution from the ultrafine to coarse size range. Total particle number concentration was measured by an Airmodus A20 for particles larger than 10 nm at 1-second resolution. This provided a continuous record of integrated aerosol number concentration to compare with size-distribution-derived counts. A Cloud Condensation Nuclei counter (CCNc, Droplet Measurement Technologies) was used to quantify CCN concentrations at controlled supersaturation levels. The CCNc alternated

https://doi.org/10.5194/egusphere-2026-4869
Preprint. Discussion started: 21 August 2026

between supersaturation settings (0.1%, 0.3%, 0.5%) to measure the number of aerosol particles that can activate into cloud droplets at each supersaturation.

Aerosol chemical composition was measured by a compact-Time of Flight Aerosol Mass Spectrometer (c-ToF AMS, Aerodyne Research Inc.). The AMS measures submicron aerosol composition (organics, sulfate, nitrate, ammonium, chloride). The compact time-of-flight AMS was operated in cycles of mass spectrum (MS) and particle time-of-flight (PToF) modes, yielding 1-minute average concentrations of non-refractory PM_1 and their composition. This instrument provided detailed insight into the chemical makeup of the marine aerosol. All collected aerosol data were corrected for hygroscopic growth where relevant.

Volatile organic compounds (VOCs) were measured by a high-resolution proton-transfer-reaction time-of-flight mass spectrometer (Aerodyne VOCUS PTR-MS). After splitting from the common inlet line, the remaining sample line leading to VOCUS PTR-MS was heated to avoid condensation in the sampling line. VOC measurements are crucial for understanding biogenic emissions from the reef (such as coral-produced sulfur compounds) and any anthropogenic influences.

Several gas-phase species were measured to provide context on sources and atmospheric chemistry. A Li-Cor LI-840A analyzer measured CO_2 (non-dispersive infrared detection), an O_3 monitor measured ozone (O_3, 9810B, Ecotech Pty Ltd.) via UV absorption, and a NOx chemiluminescent analyzer measured oxides of nitrogen (NO and NO_2, 9841A, Ecotech Pty Ltd.). All gas monitors recorded data at 1-second resolution. These gases help identify pollution events (e.g. combustion sources via CO_2 and NO_x) and provide information on photochemical activity (O_3 levels). Refractory black carbon mass was monitored by two instruments – a Tricolor Absorption Photometer (TAP, Brechtel) and a Magee Scientific Aethalometer (model AE31). Both measure light absorption by particles on a filter (at multiple wavelengths) to infer BC concentration in real time. The Aethalometer operated at 7 wavelengths (370–950 nm) on a 5-minute time base, while the three-wavelength TAP provided complementary absorption data at 1-second resolution.

A weather station (Gill MaxiMet GMX501, Gill Instruments Ltd.) mounted on the station roof provided meteorological parameters including wind speed and direction, air temperature, relative humidity (RH) and barometric pressure. Rainfall data was retrieved from the AIMS weather tower on Heron Island. Additionally, temperature/RH probes (Vaisala HMP60) were installed in the aerosol inlet line to monitor conditions inside the sampling system. One HMP60 sensor measured T/RH immediately after the aerosol dryer, and a second sensor monitored ambient T/RH before the dryer, allowing calculation of drying efficiency and humidity conditions experienced by the aerosol sample.

2.3. Data Processing and Calibration

Regular maintenance and calibration activities were performed throughout the campaign. Daily zero checks and flow checks were conducted. During these checks, the inlet line was briefly disconnected or filtered (drawing zero air or room air) and those periods have been

https://doi.org/10.5194/egusphere-2026-4869
Preprint. Discussion started: 21 August 2026

removed from the final datasets. Additional key data processing steps and calibration procedures are outlined below.

The losses in the aerosol inlet were calculated based on standard aerosol loss formulas (Baron and Willeke, 2001; Hinds, 1999). The losses accounted for included diffusional and gravitational losses as well as bend and contraction losses, which were calculated for their flow regimes, determined based on calculated Reynolds numbers. The calculated efficiency of particle penetration for different particle sizes is shown for APS and SEMS in Fig. S1-2. The SEMS and APS provided overlapping size distributions in the ~700–800 nm range. To create a single continuous particle size distribution from ~5 nm up to 2 µm, we merged the two datasets. First, APS aerodynamic diameters were converted to mobility-equivalent diameters. We assumed a representative aerosol particle density of ~1.3 g/cm^3 (sea-salt-dominated at 50% RH) and applied the equation from DeCarlo et al. (2004) to get mobility-equivalent diameters. Both SEMS and APS distributions were then corrected for the sample RH difference: since the aerosol was dried to ~50% RH in the inlet, whereas ambient humidity can be higher, we adjusted the measured diameters to "ambient equivalent" diameters using a hygroscopic growth factor model (assuming primarily ammonium sulfate/sea salt composition). Finally, in the overlapping size region we used a Tikhonov regularization approach to smoothly join the SEMS and APS data. The merged distribution was used for computing integrated aerosol properties and for visualizing size spectra.

Total aerosol number concentration was corrected for detection efficiency and any obvious false spikes (e.g., electrical noise spikes) in the CPC time series were removed. CCNc data required processing due to its supersaturation stepping. The instrument cycled through supersaturation (SS) settings of 0.5%, 0.3%, and 0.1% (each held for 10 minutes). To ensure steady state, we discarded the initial warm-up period at each new setting (specifically, the first 90 s at 0.5% SS, 150 s at 0.3%, and 240 s at 0.1% SS). The remaining CCN concentrations were averaged for each SS level interval. CCN concentrations at 0.3% SS were chosen for further analysis as 0.3% SS is likely the closest to a true supersaturation in the clouds (Horchler et al., 2025). We then derived CCN spectra (CCN concentration vs. supersaturation) for selected periods and calculated the activation ratio (CCN/CN ratio) at each supersaturation as a function of time.

The AMS data were processed with standard AMS software (SQUIRREL/PIKA in Igor Pro). Periods when the AMS was not sampling (e.g., during tuning or background check) were removed. The instrument was also re-tuned on 12 November after noticing sensitivity loss. As a result, we split the AMS dataset into two segments (pre-12 November and post-12 November) and applied the respective calibration values to each period. This ensures the reported mass concentrations are accurate throughout.

In order to account for changes in the sensitivity of the VOCUS PTR-MS, both background and calibration measurements were collected daily. On 18.11.2025 the tuned settings reset to previous values leading to the step change in sensitivity and background measurements. The detection limits (DL) were calculated for each calibrant before and after change of

https://doi.org/10.5194/egusphere-2026-4869
Preprint. Discussion started: 21 August 2026

settings and if the results were comparable the higher value of DL was used throughout the campaign (Table S2).

The raw absorption data from the Aethalometer (AE31) were corrected for known artifacts. Specifically, after each filter tape advance the AE31 would report zero or near-zero readings for a short period; these points were removed from the dataset. Additionally, a flow correction was applied. Although the AE31 was set to a nominal 2.0 L/min, the actual flow was ~1.6 L/min during operation, so we scaled the BC concentrations accordingly to reflect the true sampling volume. The Brechtel TAP data (which are inherently at 1-s resolution and lower noise) were averaged to 5-min for comparison to the Aethalometer and corrected for spot loading effects using the manufacturer's algorithm.

Quality control was performed on all data streams: obviously erroneous data (e.g., negative particle counts, sensor outages) were removed or flagged.

2.4. Calculations

To further support the work presented in this paper, several parameters were calculated. The black carbon concentration (threshold of 0.45 μg/m^3) was used to identify data strongly influenced by the local anthropogenic emissions. The identified data was marked with a pollution flag and not used in further analysis.

The Hoppel minimum (Hoppel et al., 1985; Noble and Hudson, 2019) defined as the diameter where the minimum concentration occurs between Aitken and accumulation modes, was calculated by finding the minimum diameter of a smoothing spline that was fitted to the size distribution between 40 and 140 nm. In cases when the minimum diameter was found on the edge of the studied range (40 or 140 nm), the size distribution was considered not to have a Hoppel minimum present. Additionally, the calculation of the Hoppel minimum was constrained by the previous value based on the assumption that the Hoppel minimum changing by more than 10 nm in 15 minutes is either unrealistic or a sign of a rapid change in air masses.

The CCN activation ratio was calculated as a ratio between CCN and total aerosol number concentrations. The critical diameter is defined as a diameter above which particles are assumed to activate as CCN. The critical diameter was calculated as a diameter above which the reverse sum of the particle size distribution concentration matches the CCN concentration (Sihto et al., 2011).

The 72-hour back trajectories were calculated per hour using the Hybrid Single-Particle Lagrangian Integrated Trajectory (HYSPLIT) model (Stein et al., 2015). The Lagrangian dispersion model developed by the National Oceanic and Atmospheric Administration (NOAA) was used to determine the pathway that air masses took before arriving at the sampling location. The Global Data Assimilation System (GDAS) dataset at 1° spatial resolution provided by NOAA was used for HYSPLIT analysis. Based on the calculated back trajectories, a reef fraction was calculated as the fraction of time that air masses spend over the GBR reef area during 12-hour time window before arriving at the station. The reef

https://doi.org/10.5194/egusphere-2026-4869
Preprint. Discussion started: 21 August 2026

locations were retrieved from reef mappings provided by the Great Barrier Reef Marine Park Authority (Great Barrier Reef Marine Park Authority, 2007).

The cloudiness parameter was calculated as a ratio of global radiation to the theoretical maximum radiation arriving at Heron Island (Dada et al., 2017). The theoretical maximum radiation is estimated based on the latitude of the Heron Island and the seasonal solar cycle. The cloudiness parameter lower than 0.3 represents a complete cloud cover, while values above 0.8 can be categorized as clear-sky conditions.

3. Results and discussion

3.1. Overview

Our dataset consists of two periods representing distinct meteorological regimes (Fig. 2). The first period, spanning from the beginning of the campaign until midnight on 18 November, is characterized by predominantly northerly winds, higher median relative humidity, temperature, and dew point, as well as notably lower wind speeds (median < 2 m/s) and less frequent clear-sky conditions. After this time, conditions shift to a more stable trade-wind regime, with air masses arriving primarily from the southeast. This transition is also evident in air-mass back trajectories, which show a clear shift from north–northeast marine transport during the first period to predominantly southeast marine transport thereafter (Fig. 2).

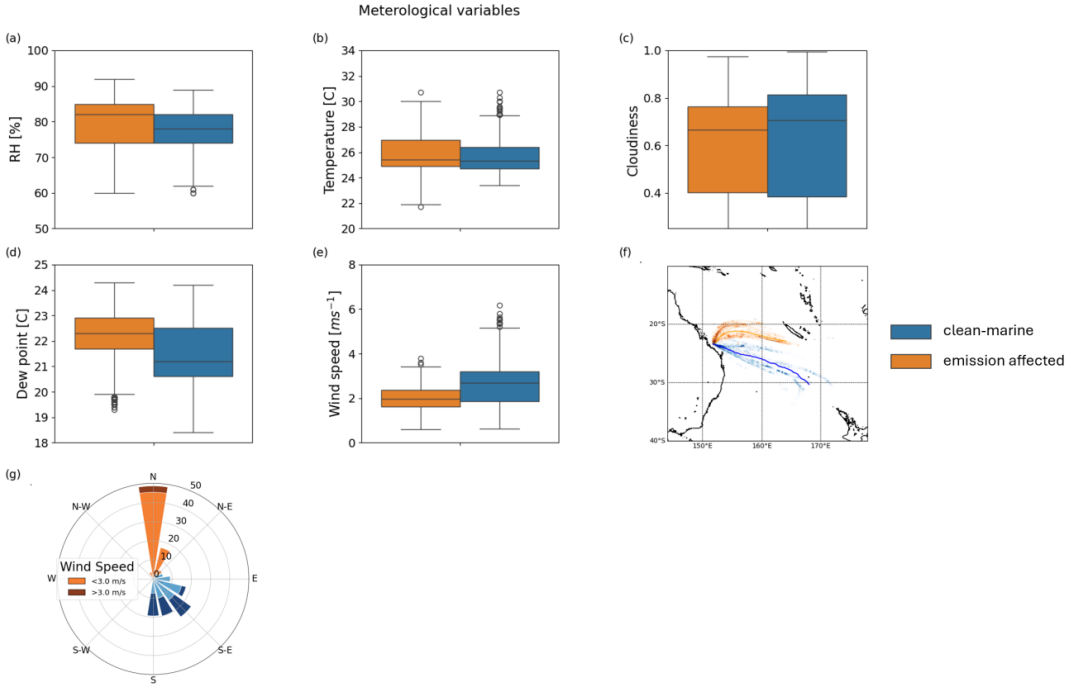

Figure 2: The meteorological regimes during the first (orange) and second (blue) time periods

https://doi.org/10.5194/egusphere-2026-4869
Preprint. Discussion started: 21 August 2026

of the campaign showing the RH (a), temperature (b), cloudiness parameter (c), dew point (d), wind speed (e), air mass history (f), and wind direction (g).

These two regimes exhibit markedly different aerosol characteristics (Fig. 3). During the first period, aerosol number concentrations are substantially elevated, with median total particle number concentrations around 600 cm^{-3} compared to approximately 200 cm^{-3} during the second period. All particle size modes show higher concentrations during the first period. We therefore refer to the first period as the emissions affected period and the second period as the clean marine period. Aerosol chemical composition shows some small changes, with the emission affected period exhibiting higher organic and sulfate and lower ammonium concentrations and fractions compared to the clean marine period (Fig. S3-4). The CCN concentrations are also enhanced, with median values near 200 cm^{-3} compared to below 100 cm^{-3} during the second period. The CCN activation ratio (CCN/CN) displays greater variability during the first period, particularly toward lower values. Such variability may indicate a larger fraction of particles that are either too small to activate at the measurement supersaturation or exhibit lower hygroscopicity due to increased organic content.

In addition, the Hoppel minimum occurs at significantly larger diameters during the first period (>100 nm) compared to approximately 80 nm during the second period (starting on 19 November). The Hoppel minimum reflects the size threshold separating particles that have undergone cloud processing from those that have not (Hoppel et al., 1985; Hoppel and Frick, 1990). A shift toward larger diameters suggests that particles required larger sizes to activate as cloud droplets, which is commonly associated with lower hygroscopicity or lower cloud supersaturation conditions (Dusek et al., 2006; McFiggans et al., 2006). It is also possible that the air masses contain more aged aerosols that were not cloud processed as recently.

Taken together, these observations indicate that the aerosol population during the first period was more variable and likely influenced by additional particle sources or precursor environments compared to the cleaner marine conditions observed during the second period. This interpretation is supported by air-mass history, which shows that during the first period air masses spent significantly more time over the GBR and surrounding reef islands before reaching Heron Island (Fig. 2a). Such transport pathways may enhance the influence of both marine biogenic emissions and local island activities, leading to increased variability in aerosol concentrations (Fig. 3) and composition (Fig. S3-4).

https://doi.org/10.5194/egusphere-2026-4869
Preprint. Discussion started: 21 August 2026

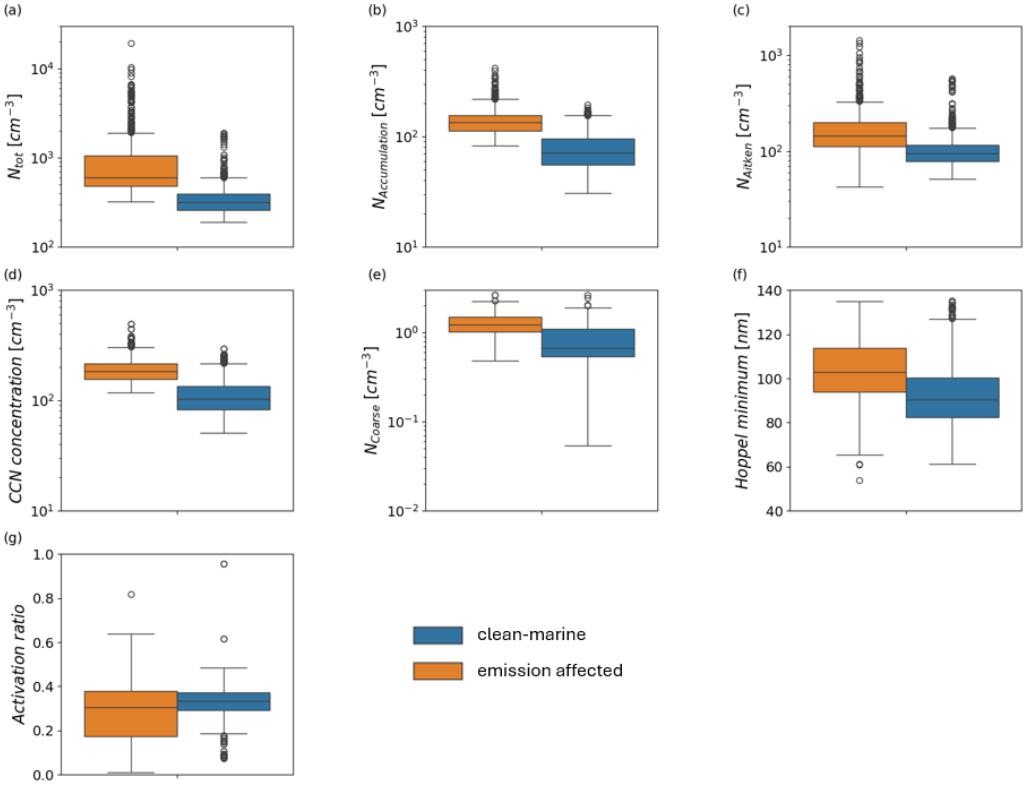

Figure 3: The total particle number concentration (N_{tot}) (a), accumulation mode concentration (b), Aitken mode concentration (c), CCN concentration (d), coarse mode concentration (e), Hoppel minimum (f) and activation ratio (g) in the two periods of the data set.

https://doi.org/10.5194/egusphere-2026-4869
Preprint. Discussion started: 21 August 2026

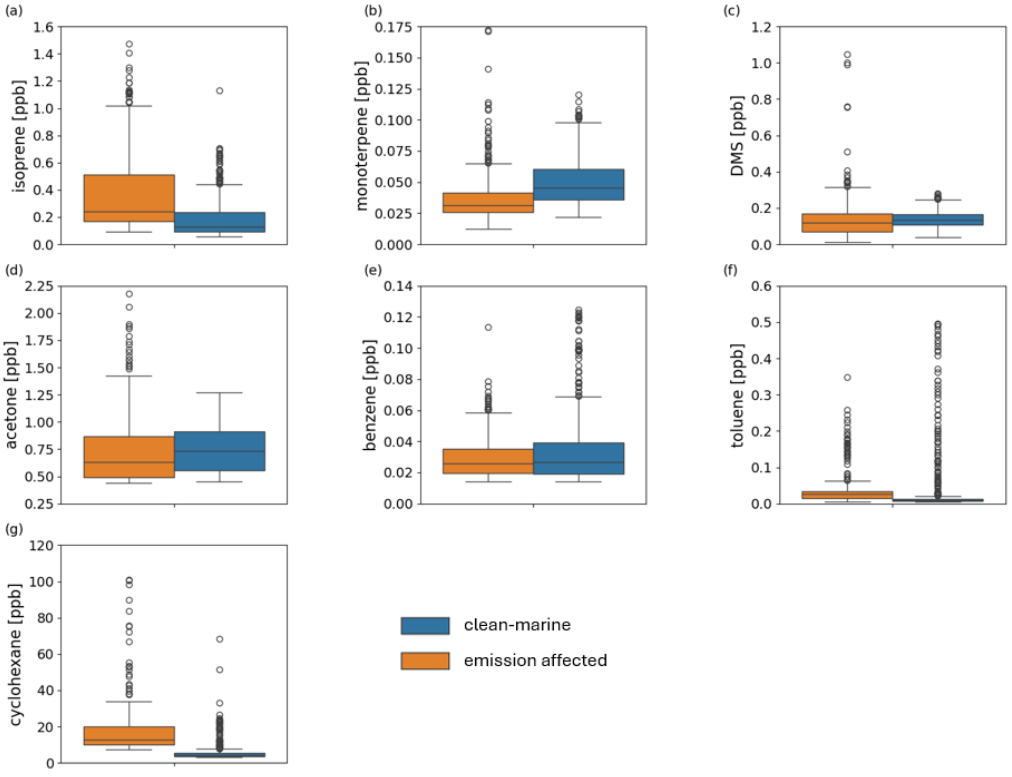

Figure 4: The concentrations of isoprene (a), monoterpene (b), DMS (c), acetone (d), benzene (e), toluene (f) and cyclohexane (g) in the two periods of the data set.

Looking at the gas-phase compounds, the concentrations of isoprene, cyclohexane and toluene are elevated during first period (Fig. 4a,f,g). Isoprene is most likely originating from local organic sources such as vegetation, while cyclohexane and toluene are possibly coming from an anthropogenic source on the island. Interestingly, the concentrations of monoterpene, DMS, and acetone are statistically higher ($p < 0.001$) during the second period (Fig. 4b) when the air spends minimum time over the island (Fig. 2a,d), suggesting biogenic marine origin such as corals or phytoplankton (Shaw et al., 2010; Swan et al., 2016; Yassaa et al., 2008). Previous research (Deschaseaux et al., 2025; Shaw et al., 2010; Swan et al., 2016; Yassaa et al., 2008) has suggested that corals also emit small concentrations of isoprene together with monoterpenes, but the isoprene emissions from local trees are much stronger and likely mask this effect.

3.2. Nanoparticle ranking

We applied nanoparticle ranking analysis (Aliaga et al., 2023) to our dataset, in order to study the contribution of local particle formation and growth to the aerosol size distribution. Our analysis reveals three distinct Gaussian modes—g1, g2, and g3 (Fig. S5)—each representing a characteristic level of NPF intensity.

https://doi.org/10.5194/egusphere-2026-4869
Preprint. Discussion started: 21 August 2026

The first mode, g1, from here on called the non-event mode, accounts for approximately one third of the 15 days of complete data and corresponds to days with negligible or absent NPF activity. As shown in Fig. 5a, the median diurnal particle size distribution for non-event days lacks any sustained growth features, instead displaying two faint sharp spikes in particle concentration across a wide size range before 06:00 and again around 18:00, suggestive of transient pollution events rather than nucleation.

The second mode, g2, from here on called the undefined mode, is found in only a fifth of the dataset. However, undefined days show a clear midday growth event and a secondary growth period in the evening (Fig. 5b). Notably, the evening mode does not appear to connect to the sub-2 nm molecular size range (Fig. 5b), indicating it likely does not originate from a nucleation process but rather from the growth of existing particles, potentially linked to local combustion emissions.

In contrast, days in the third Gaussian, g3, from here on called the NPF event mode, represent the strongest NPF events and are characterized by three distinct growth episodes. The first event occurs shortly after sunrise (05:00), another near 11:00, and a third around 17:00 (Fig. 5c). These events show sustained growth from the smallest detectable sizes. The last event terminates abruptly near sunset, emphasizing the central role of photochemistry in driving particle growth. The abrupt termination could not be explained by a shift in wind direction, leaving solar chemistry as the most likely reason for it.

Airmass history provides context for interpreting the nanoparticle ranking analysis. As shown in Fig. 2, airmasses during the period in which NAIS data are available predominantly originated from the east, indicative of a clean marine background. However, distinct differences emerge in the trajectories near Heron Island across the three modes (Fig. 6). For non-event days, airmasses approach almost directly from the east, spending minimal time over the GBR (Fig. 6b). In contrast, undefined days exhibit a modest northerly arc, with air passing over more of the reef system (Fig. 6d). Most notably, during NPF event days, airmasses take a pronounced turn northward before arriving at Heron Island, frequently traveling along the main reef chain (Fig. 6dc). Despite these distinctions, all airmasses regardless of mode pass directly over Heron Island itself, indicating that potential terrestrial influences from the island are common in all cases.

The meteorological conditions associated with each nanoparticle ranking mode show subtle distinctions that may influence new particle formation. As shown in Fig. 7d, diurnal temperature profiles are broadly similar, but non-event days exhibit slightly lower midday temperatures, possibly reflecting increased cloudiness or higher aerosol loading suppressing surface heating. In contrast, undefined days show cooler nighttime temperatures, which may indicate more efficient radiative cooling under clearer skies.

https://doi.org/10.5194/egusphere-2026-4869
Preprint. Discussion started: 21 August 2026

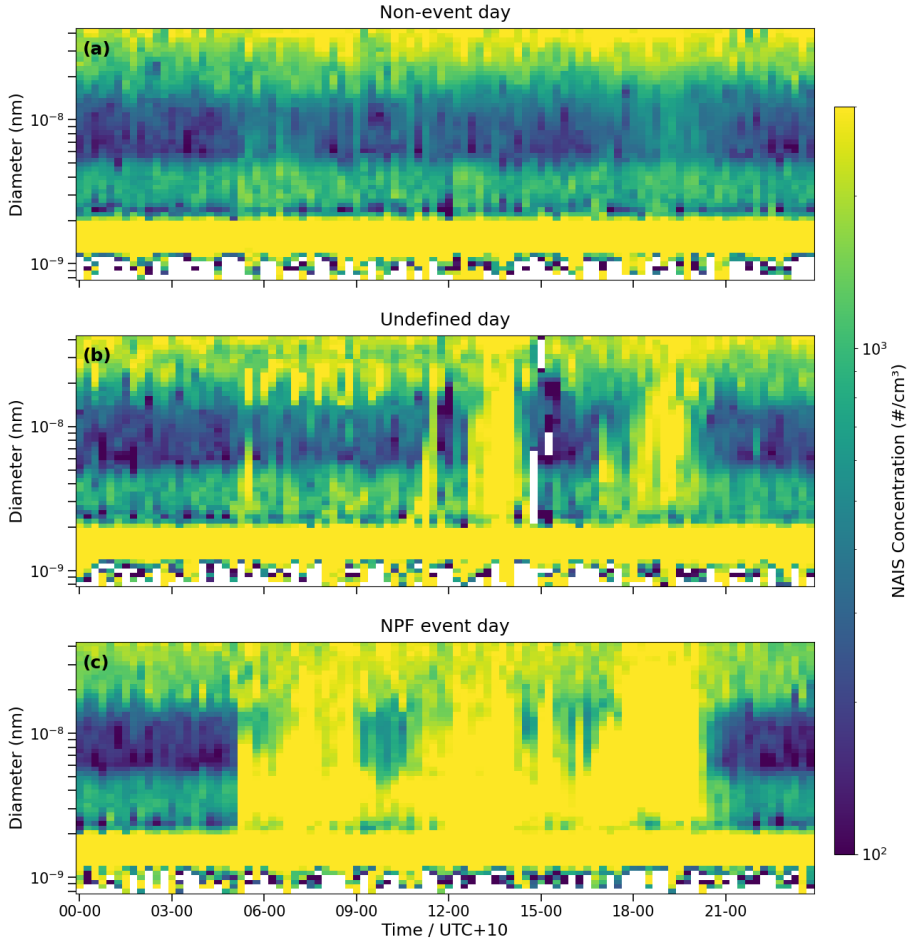

Figure 5: Diurnal variation of the median particle number size distribution measured during non-event day (a), undefined day (b), and NPF event day (c).

375

https://doi.org/10.5194/egusphere-2026-4869
Preprint. Discussion started: 21 August 2026

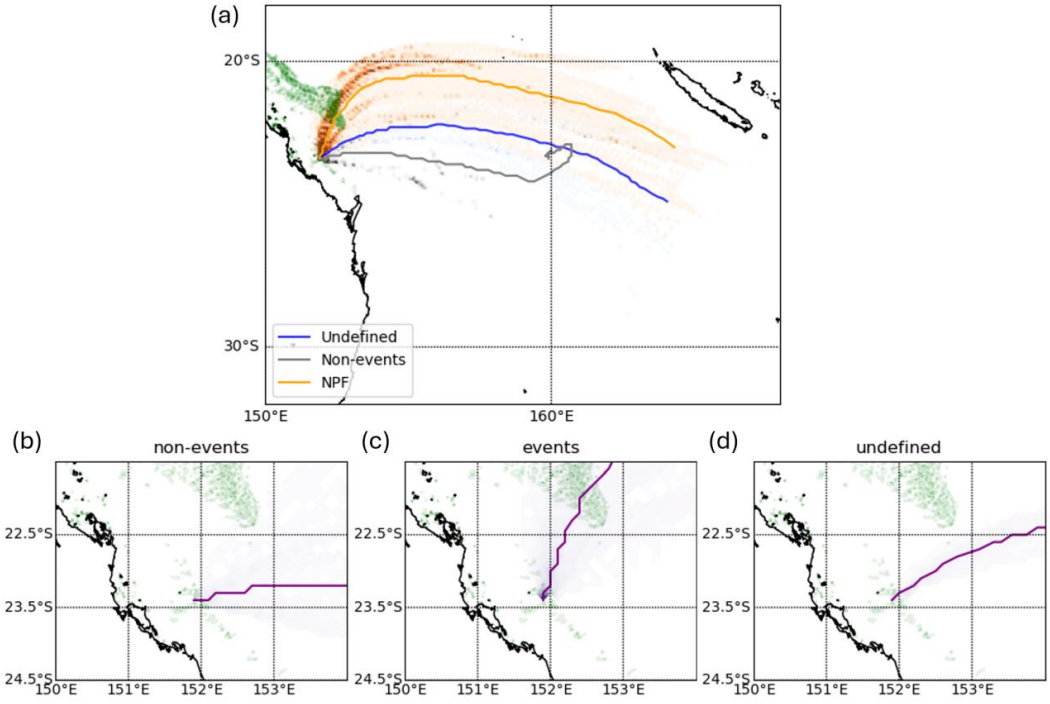

Figure 6: The air mass history for NPF event days (a,c), undefined days (a,d), and non-event days (a,b). Color intensity shows the frequency of trajectory overpass for each pixel during the analyzed period, with the solid line denoting the average trajectory. The green contours (b-d) show locations of coral reefs in the GBR.

Solar radiation profiles support this as well as the cloudiness parameter (Fig. 7f and S6), with both indicating clearer skies on undefined and NPF event days. Notably, undefined days tend to receive more morning solar radiation (Fig. 7f), suggesting earlier onset of photochemical activity, though this does not always lead to particle formation. Wind speed is also lower on average during these days (Fig. 7a), likely contributing to lower vertical mixing and slower replenishment of precursors. In contrast, the NPF event days exhibit slightly lower atmospheric pressure likely resulting in better vertical mixing and a higher solar radiation (Fig. 7b,f), which, in combination with observed wind direction changes aligning with airmass history, may create conditions more conducive to particle growth. These patterns suggest that the subtle interplay between radiation, moisture availability, and boundary layer dynamics could play a role in modulating event likelihood.

Condensation sink (CS) is a well-established regulator of NPF, as pre-existing aerosol surface area can effectively scavenge low-volatility vapors before they contribute to nucleation or growth (Kerminen et al., 2018; Kulmala et al., 2001). Over the GBR, CS values are typically very low, typically below 4×10^{-4} s^{-1} (Fig 7i-k), but our analysis reveals distinct patterns across nanoparticle ranking modes, indicating a delicate balance between suppression and source-driven variability (Fig. 7i-k). On non-event days, CS values are

https://doi.org/10.5194/egusphere-2026-4869
Preprint. Discussion started: 21 August 2026

typically 3×10^{-4} s^{-1}, coinciding with consistently low nucleation mode concentrations (<300 cm^{-3}, Fig 7i), suggesting that even relatively modest sinks in this clean marine environment can effectively hinder particle formation. In contrast, both undefined and NPF event days show similarly low median CS values (about 1.5×10^{-4} s^{-1}), yet markedly different outcomes in nucleation mode concentrations (Fig. 7j,k). On undefined days, concentrations remain moderate (250–350 cm^{-3}), while event days exhibit a broader range extending up to 1200 cm^{-3}. This divergence implies that differences in aerosol sink alone cannot account for the variability in NPF intensity and instead points toward variability in precursor vapor availability or nucleation conditions. Compared to continental or polluted coastal environments, where CS frequently exceeds 1×10^{-3} s^{-1} and can strongly suppress NPF (Nieminen et al., 2018; Wang et al., 2021), the GBR represents a regime where even subtle changes in CS may modulate particle formation efficiency, but source dynamics likely play the dominant role in controlling event strength.

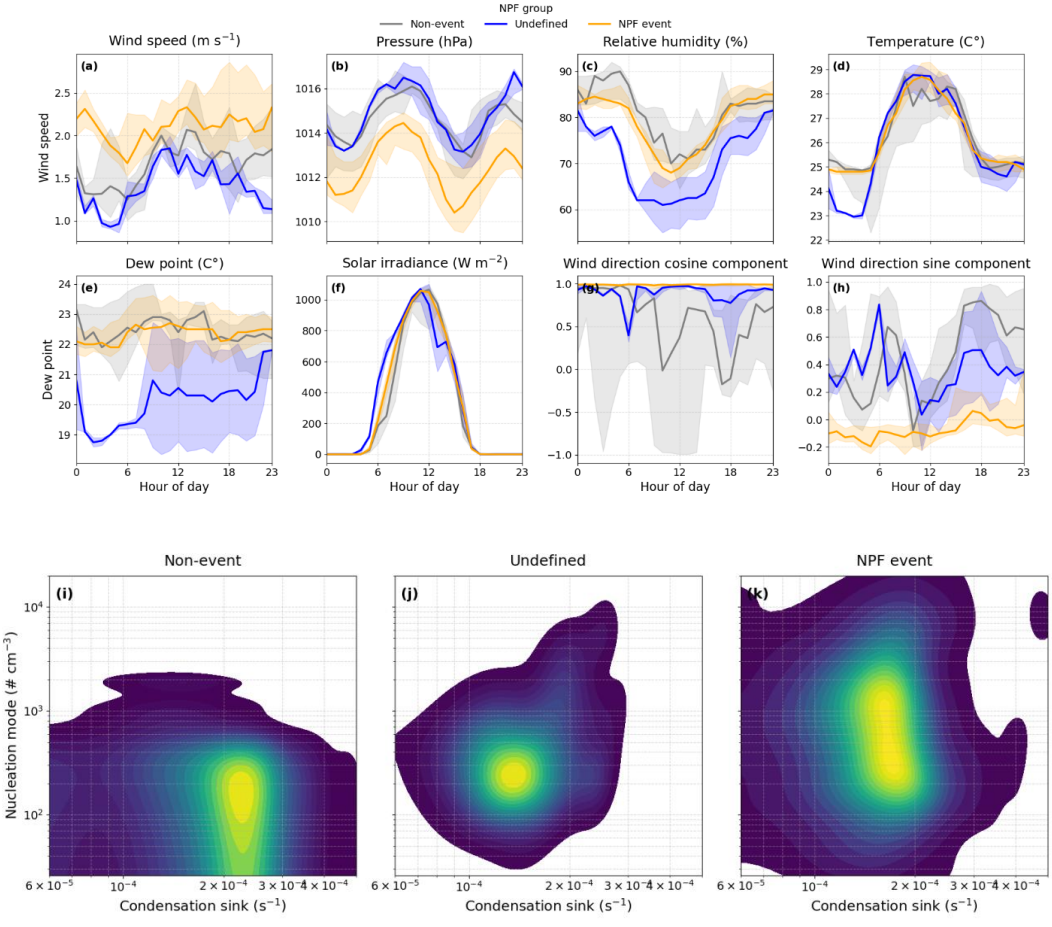

Figure 7: Diurnal variation of metrological variables: wind speed (a), pressure (b), relative humidity (c), temperature (d), dew point (e), solar radiation (f), wind direction cosine (g) and

https://doi.org/10.5194/egusphere-2026-4869
Preprint. Discussion started: 21 August 2026

sine (h) component during NPF event days (yellow), undefined days (blue), and non-event days (grey). Median values are shown by a straight line, while shaded areas present the interquartile ranges. Subplots i-k present the relation between condensation sink and nucleation mode measured with NAIS for non-event days (i), undefined days (j), and NPF event (k). This relationship is presented as relative densities (kde); hence the color scale does not represent absolute values and is irrelevant for the interpretation.

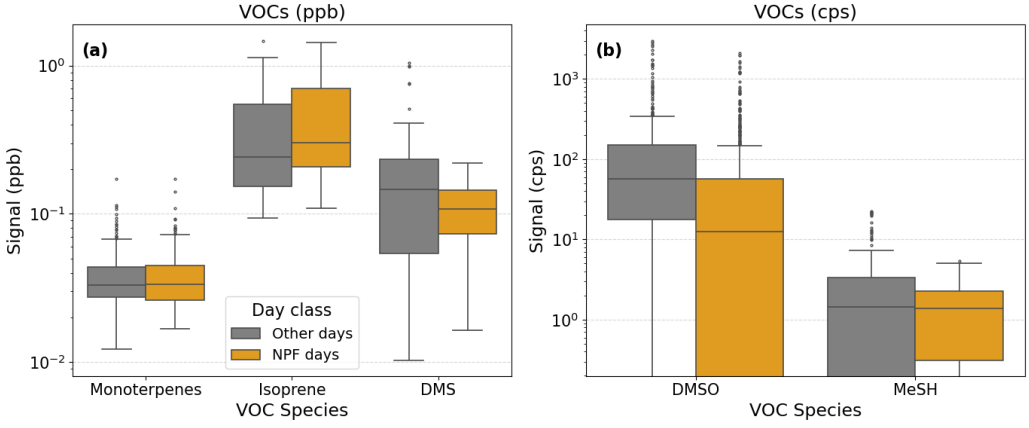

Figure 8: Boxplots of VOC concentrations measured on the NPF event days (yellow) and combined data for undefined and non-event days (other days, grey). Subplots (a) presents calibrated data in ppb unit while subplot (b) shows data as counts per seconds (cps).

Our observational data show that days with NPF events coincide with elevated isoprene levels, while DMS and its oxidation product DMSO are notably lower than on non-event days (Fig. 8). Due to lack of VOC data for most undefined days, we have combined non-event and undefined days under the term other days for the rest of this analysis. It can be hypothesized that the lower DMS concentrations are due to photochemical oxidation during clear sky days. Coral reef VOC emissions (such as DMS and monoterpenes) are known to be capable of producing new aerosol particles in the marine boundary layer, but the occurrence of NPF even when DMS/DMSO are relatively low and its absence when they are higher challenges the simple view that more DMS invariably means stronger nucleation. Instead, these results support the emerging understanding that NPF in pristine environments requires a combination of precursors and favorable conditions: for example, nucleation in clean marine air may involve a mixture of sulfur species with ammonia, amines, or halogenated compounds (e.g. iodine emissions) to stabilize new cluster formation (Kirkby et al., 2011; O'Dowd et al., 2002; Sipilä et al., 2016).

https://doi.org/10.5194/egusphere-2026-4869
Preprint. Discussion started: 21 August 2026

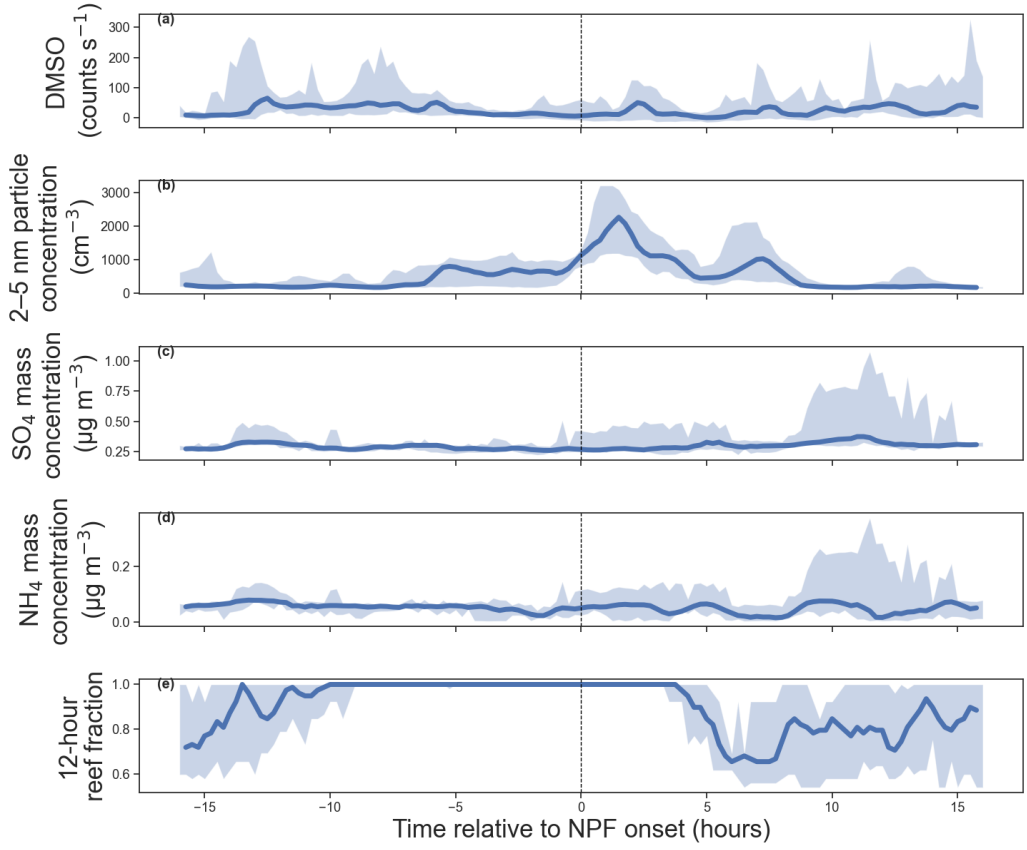

440 Figure 9: Timeseries of concentration of DMSO, 2-5 nm particle concentration, sulfate (SO_4), and ammonium (NH_4) as well as 12-hour reef fraction relative to the NPF onset. Median values are shown by a straight line while shaded areas present the interquartile ranges.

Figure 9 shows the median time series of DMSO, nanoparticle number concentrations (2–5 nm), and aerosol sulfate and ammonium mass concentrations relative to the onset of NPF. 445 Onset is defined here as the increase of the 2 – 5 nm particle number concentration above the 75th quantile for a minimum of 30 minutes. This method detects a maximum of three NPF events a day in our dataset, consistent with visual inspection of the data (Fig. 5). DMSO concentrations are highest during the hours preceding NPF events and decrease gradually toward the time of onset (Fig. 9a). The concentrations of 2–5 nm particles increase sharply 450 at the onset of NPF as expected and remain elevated for several hours afterward (Fig. 9b), indicating sustained nucleation or early particle growth during the daytime photochemical period. Sulfate mass concentrations do not increase immediately at the onset of particle formation but instead rise several hours later (Fig. 9c). Ammonium follows a similar pattern (Fig. 9d), suggesting both ammonium and sulfate or their precursors participate in particle 455 formation and growth. This temporal sequence of declining DMSO, followed by nanoparticle

https://doi.org/10.5194/egusphere-2026-4869
Preprint. Discussion started: 21 August 2026

formation, and subsequently increasing sulfate and ammonium mass—is consistent with the oxidation of reduced sulfur compounds leading to sulfuric acid production and particle growth. Finally, airmass back trajectory analysis shows that the fraction of time the airmasses spent over the GBR itself tends to increase towards unity about 10 hours prior to onset and remain high until several hours after NPF (Fig. 9e), suggesting that sources at the GBR, be they reefs, vegetation or anthropogenic sources, affect the initiation of NPF. This behaviour is also specific and enhanced during NPF days, as DMSO concentrations are elevated particularly on nights prior to NPF event days and airmasses spent significantly more time over the reef during NPF days (Fig S7).

The observation that DMSO concentrations decline approaching NPF onset indicates that the events are not triggered by elevated concentrations of this compound itself, but rather by chemical conversion of a precursor pool accumulated during the preceding night. The several-hour delay between nanoparticle formation and detectable increases in sulfate mass is consistent with the time required for newly formed clusters to grow (Kulmala et al., 2001, 2004) into the size range detectable by AMS (over ~50–70 nm). Together, these observations support a mechanism in which DMSO accumulates overnight in the marine boundary layer (Fig. S7) and is subsequently oxidized during the daytime photochemical period, producing sulfuric acid that drives nanoparticle formation and growth. Overall S-containing VOC tend to have higher counts during other than NPF days (Fig S8), highlighting that sulfur availability alone may not be the limited factor the NPF, but rather the combination of sulfur availability and sulfur processing via photochemistry. The decline in DMSO prior to NPF onset therefore likely reflects the progression of sulfur oxidation chemistry rather than depletion by particle condensation alone. Similar precursor-conversion dynamics have been observed in other marine environments where biogenic sulfur emissions play a central role in particle formation processes (Barnes et al., 2006; Berndt et al., 2023), suggesting that coral reef ecosystems may represent a locally important and previously under-characterized source region for sulfur-driven aerosol formation. Previous studies have suggested that coral reefs DMS emissions may not contribute a major component to particle number concentrations in large spatial scales, but they may still have an impact on a smaller spatial scale (Fiddes et al., 2022; Jackson et al., 2022).

Organic aerosol composition was examined using the AMS f44–f43 framework (Ng et al., 2010). The aerosol occupy the highly oxidized region of the triangle throughout the campaign (Fig. S9), indicating that the organic aerosol is dominated by aged-oxygenated components. During nucleation periods the median composition shifts slightly toward higher f43 and lower f44 (Fig. S9-10), suggesting the presence of somewhat less oxidized secondary organic aerosol. However, the aerosol remains highly oxidized overall (f44 > 0.22), inconsistent with fresh primary emissions. The shift to mildly less oxidized background aerosol suggests that we are likely observing a change in the background conditions towards more active photochemistry or increased production of newly oxygenated VOCs.

VOC analysis reveals that the overall VOC composition remains broadly similar between nucleation and non-event days (Fig. S11). NPF days show enhanced signal intensity for oxygenated hydrocarbons during the morning and midday period (Fig. S8 and S11). This

https://doi.org/10.5194/egusphere-2026-4869
Preprint. Discussion started: 21 August 2026

indicates increased oxidation of the existing VOC pool rather than the introduction of distinct precursor compounds. The non-event days show higher median concentrations of $C_4H_9^+$ ion, except at 9 and 10 a.m. when its concentration is higher during NPF events (Fig. S12). The $C_4H_9^+$ is a common fragmentation ion that most likely comes from more than one compound. Although the difference in $C_4H_9^+$ signal during NPF is the most noticeable one, overall S-, and N-containing compounds show lower concentrations on NPF event days (Fig. S8). This can suggest stronger influence of nitrogen oxide chemistry on days without NPF events, which can suppress NPF (Wildt et al., 2014; Zhao et al., 2018). Our analysis indicates that NPF and the remaining days share a broadly similar VOC composition space, suggesting that nucleation is not triggered by big changes in precursor vapour composition. Instead, the main difference lies in the relative abundance and timing of oxygenated species, consistent with stronger oxidation and precursor processing on NPF days.

4. Conclusions

Our results highlight the strong influence of regional transport and air-mass residence time over the GBR on aerosol properties and particle formation dynamics. Two distinct regimes were observed during the campaign. The first period was characterized by air masses arriving from the north and northeast that travelled along the main reef chain before reaching Heron Island. During this period, particle number concentrations were substantially higher and aerosol properties were more variable, suggesting the influence of multiple particle sources or precursor environments. In contrast, the second period was dominated by southeasterly trade winds, representing a cleaner marine regime in which air masses spent most of their transport time over the open Pacific Ocean before arriving at the site. This regime was associated with lower aerosol concentrations and more stable aerosol properties. Because both regimes originate from the eastern Pacific sector, these observations suggest that increased residence time over the continental shelf and the reef system enhances both particle number concentrations and the complexity of aerosol dynamics. Air mass trajectories also indicate that NPF event days were associated with transport pathways that followed the reef chain before reaching Heron Island, suggesting that processes occurring within the reef environment may influence the availability of particle precursors.

The strength of NPF events appears to follow patterns commonly observed in other environments, where particle formation is controlled by a combination of meteorological conditions, precursor availability, and the magnitude of the condensation sink. Non-event days were generally characterized by higher condensation sinks and increased cloudiness, which likely reduced photochemical activity and resulted in higher concentrations of less-oxidized VOCs such as DMS, DMSO, and methanethiol. NPF event days displayed multiple growth episodes beginning shortly after sunrise and continuing throughout the daytime photochemical period. Both undefined and event days exhibited similarly low condensation sinks and lower concentrations of DMS, DMSO, and methanethiol, consistent with enhanced photochemical processing. The remaining differences in NPF intensity between undefined and event days are therefore likely driven by additional factors, such as the

https://doi.org/10.5194/egusphere-2026-4869
Preprint. Discussion started: 21 August 2026

availability of co-condensing vapors or subtle meteorological differences including wind speed, wind direction, and air-mass history.

Trace gas and chemical composition measurements suggest a possible mechanism for NPF events over the reef. By aligning both DMSO and aerosol chemical composition measurements with NPF start times we show that DMSO concentrations peak prior to NPF onset, followed by NPF onset and increase in 2 – 5 nm particles while DMSO concentrations decline. Furthermore, several hours after the onset of NPF, aerosol chemical composition measurements exhibit an increase in sulfate and ammonia mass. This temporal sequence suggests that DMSO and possibly other S-containing compounds accumulate overnight and are subsequently oxidized during the daytime photochemical period, producing sulfuric acid that contributes to particle formation and growth.

Our findings highlight the importance of coral reef environments as potential sources of aerosol precursors in otherwise clean marine atmospheres. These results support a novel constraint for regional modelling and an incorporation of biogenic aerosol processes from reef systems into Earth system models. While previous studies have suggested that reef-derived emissions may have a limited impact on regional particle number concentrations, our results indicate that they may influence particle formation at smaller spatial scales. Further work is needed to better constrain the roles of sulfur chemistry, organic oxidation products, and other potential species such as ammonia, amines, or halogen compounds in driving nucleation in reef environments. Understanding these processes is important not only for aerosol chemistry but also for assessing the potential influence of coral reef ecosystems on cloud formation and regional climate in the tropical marine atmosphere.

Code and data availability

The dataset used in this study will be available at the Zenodo repository by the publication date.

Author Contributions

M.O. and J.S. collected, processed and analyzed the data, prepared the figures and wrote the manuscript. M.O., J.S., B.M., Z.L., J.A. calibrated and tuned instruments. B.M., D.H., J.S., M.O., Z.L., J.A and Z.R. conceptualized the study. All co-authors provided comments and reviewed the manuscript.

Competing interests

The authors declare that they have no conflict of interest.

Acknowledgement

The authors would like to acknowledge the Traditional Owners of the Great Barrier Reef, particularly the groups from the PCCC TUMRA, for permission to collect atmospheric aerosol data in/on their sea Country. The atmospheric measurements that this work is based on, were carried out at Heron Island Research Station (The University of Queensland,

https://doi.org/10.5194/egusphere-2026-4869
Preprint. Discussion started: 21 August 2026

Australia). We would like to thank station staff members who helped us with conducting our research. The authors also thank Ceylena Holloway, Peter Marshall, and Pauline Graham for planning, administrative, and logistical support for the campaign.

Financial Support

This research was funded by the Reef Restoration and Adaptation Program through the partnership between the Australian Governments Reef Trust and the Great Barrier Reef Foundation.

References

Albrecht, B. A.: Aerosols, Cloud Microphysics, and Fractional Cloudiness, Science, 245, 1227–1230, https://doi.org/10.1126/science.245.4923.1227, 1989.

Aliaga, D., Tuovinen, S., Zhang, T., Lampilahti, J., Li, X., Ahonen, L., Kokkonen, T., Nieminen, T., Hakala, S., Paasonen, P., Bianchi, F., Worsnop, D., Kerminen, V.-M., and Kulmala, M.: Nanoparticle ranking analysis: determining new particle formation (NPF) event occurrence and intensity based on the concentration spectrum of formed (sub-5 nm) particles, Aerosol Res., 1, 81–92, https://doi.org/10.5194/ar-1-81-2023, 2023.

Coral bleaching events | AIMS: https://www.aims.gov.au/research-topics/environmental-issues/coral-bleaching/coral-bleaching-events, last access: 10 February 2025.

Anthony, K. R. N., Helmstedt, K. J., Bay, L. K., Fidelman, P., Hussey, K. E., Lundgren, P., Mead, D., McLeod, I. M., Mumby, P. J., Newlands, M., Schaffelke, B., Wilson, K. A., and Hardisty, P. E.: Interventions to help coral reefs under global change—A complex decision challenge, PLOS ONE, 15, e0236399, https://doi.org/10.1371/journal.pone.0236399, 2020.

Barnes, I., Hjorth, J., and Mihalopoulos, N.: Dimethyl Sulfide and Dimethyl Sulfoxide and Their Oxidation in the Atmosphere, Chem. Rev., 106, 940–975, https://doi.org/10.1021/cr020529+, 2006.

Baron, P. A. and Willeke, K. (Eds.): Aerosol Measurement: Principles, Techniques, and Applications, 2nd ed., Wiley-Interscience, New York, 2001.

Bay, L. K., Rocker, M., Boström-Einarsson, L., Babcock, R., Buerger, P., Cleves, P., Harrison, D., Negri, A., Quigley, K., Randall, C. J., van Oppen, M. J. H., and Webster, N.: Reef Restoration and Adaptation Program: Intervention Technical Summary. A report provided to the Australian Government by the Reef Restoration and Adaptation Program, Australian Institute of Marine Science (AIMS), 2019.

Berndt, T., Hoffmann, E. H., Tilgner, A., Stratmann, F., and Herrmann, H.: Direct sulfuric acid formation from the gas-phase oxidation of reduced-sulfur compounds, Nat. Commun., 14, 4849, https://doi.org/10.1038/s41467-023-40586-2, 2023.

https://doi.org/10.5194/egusphere-2026-4869
Preprint. Discussion started: 21 August 2026

Braga, R. C., Rosenfeld, D., Hernandez, D., Medcraft, C., Efraim, A., Moser, M., Lucke, J., Doss, A., and Harrison, D.: Cloud processing dominates the vertical profiles of aerosols in marine air masses over the Great Barrier Reef, Atmos. Res., 315, 107928, https://doi.org/10.1016/j.atmosres.2025.107928, 2025.

Broadgate, W. J., Liss, P. S., and Penkett, S. A.: Seasonal emissions of isoprene and other reactive hydrocarbon gases from the ocean, Geophys. Res. Lett., 24, 2675–2678, https://doi.org/10.1029/97GL02736, 1997.

Charlson, R. J., Lovelock, J. E., Andreae, M. O., and Warren, S. G.: Oceanic phytoplankton, atmospheric sulphur, cloud albedo and climate, Nature, 326, 655–661, https://doi.org/10.1038/326655a0, 1987.

Chen, Q., Sherwen, T., Evans, M., and Alexander, B.: DMS oxidation and sulfur aerosol formation in the marine troposphere: a focus on reactive halogen and multiphase chemistry, Atmos. Chem. Phys., 18, 13617–13637, https://doi.org/10.5194/acp-18-13617-2018, 2018.

Condie, S. A., Anthony, K. R. N., Babcock, R. C., Baird, M. E., Beeden, R., Fletcher, C. S., Gorton, R., Harrison, D., Hobday, A. J., Plagányi, É. E., and Westcott, D. A.: Large-scale interventions may delay decline of the Great Barrier Reef, R. Soc. Open Sci., 8, 201296, https://doi.org/10.1098/rsos.201296, 2021.

Cropp, R., Gabric, A., van Tran, D., Jones, G., Swan, H., and Butler, H.: Coral reef aerosol emissions in response to irradiance stress in the Great Barrier Reef, Australia, Ambio, 47, 671–681, https://doi.org/10.1007/s13280-018-1018-y, 2018.

Dada, L., Paasonen, P., Nieminen, T., Buenrostro Mazon, S., Kontkanen, J., Peräkylä, O., Lehtipalo, K., Hussein, T., Petäjä, T., Kerminen, V.-M., Bäck, J., and Kulmala, M.: Long-term analysis of clear-sky new particle formation events and nonevents in Hyytiälä, Atmos. Chem. Phys., 17, 6227–6241, https://doi.org/10.5194/acp-17-6227-2017, 2017.

Deschaseaux, E., Jones, G., and Swan, H.: Dimethylated sulfur compounds in coral-reef ecosystems, Environ. Chem., 13, 239–251, https://doi.org/10.1071/EN14258, 2015.

Deschaseaux, E. S. M., Dunne, E., Schulz, K. G., Eyre, B. D., and Harrison, D. P.: The Central Great Barrier Reef as a Net Source of Climatically Relevant Biogenic Volatile Organic Compounds, J. Geophys. Res. Oceans, 130, e2024JC021192, https://doi.org/10.1029/2024JC021192, 2025.

Dietzel, A., Bode, M., Connolly, S. R., and Hughes, T. P.: The population sizes and global extinction risk of reef-building coral species at biogeographic scales, Nat. Ecol. Evol., 5, 663–669, https://doi.org/10.1038/s41559-021-01393-4, 2021.

Dusek, U., Frank, G. P., Hildebrandt, L., Curtius, J., Schneider, J., Walter, S., Chand, D., Drewnick, F., Hings, S., Jung, D., Borrmann, S., and Andreae, M. O.: Size Matters More Than

https://doi.org/10.5194/egusphere-2026-4869
Preprint. Discussion started: 21 August 2026

Chemistry for Cloud-Nucleating Ability of Aerosol Particles, Science, 312, 1375–1378, https://doi.org/10.1126/science.1125261, 2006.

Eckert, C., Hernandez-Jaramillo, D. C., Medcraft, C., Harrison, D. P., and Kelaher, B. P.: Drone-Based Measurement of the Size Distribution and Concentration of Marine Aerosols above the Great Barrier Reef, Drones, 8, 292, https://doi.org/10.3390/drones8070292, 2024.

Fiddes, S. L., Woodhouse, M. T., Utembe, S., Schofield, R., Alexander, S. P., Alroe, J., Chambers, S. D., Chen, Z., Cravigan, L., Dunne, E., Humphries, R. S., Johnson, G., Keywood, M. D., Lane, T. P., Miljevic, B., Omori, Y., Protat, A., Ristovski, Z., Selleck, P., Swan, H. B., Tanimoto, H., Ward, J. P., and Williams, A. G.: The contribution of coral-reef-derived dimethyl sulfide to aerosol burden over the Great Barrier Reef: a modelling study, Atmos. Chem. Phys., 22, 2419–2445, https://doi.org/10.5194/acp-22-2419-2022, 2022.

Fox-Kemper, B., Hewitt, H. T., Xiao, C., Aðalgeirsdóttir, G., Drijfhout, S. S., Edwards, T. L., Golledge, N. R., Hemer, M., Kopp, R., Krinner, G., Mix, A., Notz, D., Nowicki, S., Nurhati, I. S., Ruiz, L., Sallée, J.-B., Slangen, A. B. A., and Yu, Y.: Ocean, Cryosphere and Sea Level Change, in: Climate Change 2021: The Physical Science Basis. Contribution of Working Group I to the Sixth Assessment Report of the Intergovernmental Panel on Climate Change, edited by: Masson-Delmotte, V., Zhai, P., Pirani, S. L., Connors, S. L., Péan, C., Berger, S., Caud, Y., Chen, L., Goldfarb, L., Gomis, M. I., Huang, M., Leitzell, K., Lonnoy, E., Matthews, J. B. R., Maycock, T. K., Waterfield, T., Yelekçi, O., Yu, R., and Zhou, B., Cambridge University Press, Cambridge, United Kingdom and New York, NY, USA, 1211–1362, https://doi.org/10.1017/9781009157896.011, 2021.

Great Barrier Reef Marine Park Authority: Great Barrier Reef (GBR) Features, 2007.

Harris, D. L., Rovere, A., Casella, E., Power, H., Canavesio, R., Collin, A., Pomeroy, A., Webster, J. M., and Parravicini, V.: Coral reef structural complexity provides important coastal protection from waves under rising sea levels, Sci. Adv., 4, eaao4350, https://doi.org/10.1126/sciadv.aao4350, 2018.

Harrison, D. P.: An Overview of Environmental Engineering Methods for Reducing Coral Bleaching Stress, in: Oceanographic Processes of Coral Reefs, CRC Press, 2024.

Hernandez-Jaramillo, D. C., Medcraft, C., Braga, R. C., Butcherine, P., Doss, A., Kelaher, B., Rosenfeld, D., and Harrison, D. P.: New airborne research facility observes sensitivity of cumulus cloud microphysical properties to aerosol regime over the great barrier reef, Environ. Sci. Atmos., 4, 861–871, https://doi.org/10.1039/D4EA00009A, 2024.

Hinds, W. C.: Aerosol Technology: Properties, Behavior, and Measurement of Airborne Particles, 2nd ed., Wiley-Interscience, New York, 1999.

https://doi.org/10.5194/egusphere-2026-4869
Preprint. Discussion started: 21 August 2026

Hoppel, W. A. and Frick, G. M.: Submicron aerosol size distributions measured over the tropical and South Pacific, Atmos. Environ. Part Gen. Top., 24, 645–659, https://doi.org/10.1016/0960-1686(90)90020-N, 1990.

Hoppel, W. A., Fitzgerald, J. W., and Larson, R. E.: Aerosol size distributions in air masses advecting off the east coast of the United States, J. Geophys. Res. Atmos., 90, 2365–2379, https://doi.org/10.1029/JD090iD01p02365, 1985.

Horchler, E. J., Alroe, J., Harrison, L., Cravigan, L., Harrison, D. P., and Ristovski, Z. D.: Measurement report: Aerosol and cloud nuclei properties along the Central and Northern Great Barrier Reef: Impact of continental emissions , EGUsphere, 1–21, https://doi.org/10.5194/egusphere-2025-465, 2025.

Hughes, T. P., Barnes, M. L., Bellwood, D. R., Cinner, J. E., Cumming, G. S., Jackson, J. B. C., Kleypas, J., van de Leemput, I. A., Lough, J. M., Morrison, T. H., Palumbi, S. R., van Nes, E. H., and Scheffer, M.: Coral reefs in the Anthropocene, Nature, 546, 82–90, https://doi.org/10.1038/nature22901, 2017a.

Hughes, T. P., Kerry, J. T., Álvarez-Noriega, M., Álvarez-Romero, J. G., Anderson, K. D., Baird, A. H., Babcock, R. C., Beger, M., Bellwood, D. R., Berkelmans, R., Bridge, T. C., Butler, I. R., Byrne, M., Cantin, N. E., Comeau, S., Connolly, S. R., Cumming, G. S., Dalton, S. J., Diaz-Pulido, G., Eakin, C. M., Figueira, W. F., Gilmour, J. P., Harrison, H. B., Heron, S. F., Hoey, A. S., Hobbs, J.-P. A., Hoogenboom, M. O., Kennedy, E. V., Kuo, C., Lough, J. M., Lowe, R. J., Liu, G., McCulloch, M. T., Malcolm, H. A., McWilliam, M. J., Pandolfi, J. M., Pears, R. J., Pratchett, M. S., Schoepf, V., Simpson, T., Skirving, W. J., Sommer, B., Torda, G., Wachenfeld, D. R., Willis, B. L., and Wilson, S. K.: Global warming and recurrent mass bleaching of corals, Nature, 543, 373–377, https://doi.org/10.1038/nature21707, 2017b.

Hughes, T. P., Anderson, K. D., Connolly, S. R., Heron, S. F., Kerry, J. T., Lough, J. M., Baird, A. H., Baum, J. K., Berumen, M. L., Bridge, T. C., Claar, D. C., Eakin, C. M., Gilmour, J. P., Graham, N. A. J., Harrison, H., Hobbs, J.-P. A., Hoey, A. S., Hoogenboom, M., Lowe, R. J., McCulloch, M. T., Pandolfi, J. M., Pratchett, M., Schoepf, V., Torda, G., and Wilson, S. K.: Spatial and temporal patterns of mass bleaching of corals in the Anthropocene, Science, 359, 80–83, https://doi.org/10.1126/science.aan8048, 2018.

Jackson, R., Gabric, A., and Cropp, R.: Effects of ocean warming and coral bleaching on aerosol emissions in the Great Barrier Reef, Australia, Sci. Rep., 8, 14048, https://doi.org/10.1038/s41598-018-32470-7, 2018.

Jackson, R. L., Woodhouse, M. T., Gabric, A. J., Cropp, R. A., Swan, H. B., Deschaseaux, E. S. M., and Trounce, H.: Modelling the influence of coral-reef-derived dimethylsulfide on the atmosphere of the Great Barrier Reef, Australia, Front. Mar. Sci., 9, https://doi.org/10.3389/fmars.2022.910423, 2022.

https://doi.org/10.5194/egusphere-2026-4869
Preprint. Discussion started: 21 August 2026

Kerminen, V.-M., Chen, X., Vakkari, V., Petäjä, T., Kulmala, M., and Bianchi, F.: Atmospheric new particle formation and growth: review of field observations, Environ. Res. Lett., 13, 103003, https://doi.org/10.1088/1748-9326/aadf3c, 2018.

Khan, S. B., Alroe, J., Medcraft, C., Sauret, E., Harrison, D., and Ristovski, Z.: Secondary droplet breakup of impaction-pin nozzle: Comparison between experimental and CFD-DPM modelling, J. Aerosol Sci., 190, 106664, https://doi.org/10.1016/j.jaerosci.2025.106664, 2025.

Kirkby, J., Curtius, J., Almeida, J., Dunne, E., Duplissy, J., Ehrhart, S., Franchin, A., Gagné, S., Ickes, L., Kürten, A., Kupc, A., Metzger, A., Riccobono, F., Rondo, L., Schobesberger, S., Tsagkogeorgas, G., Wimmer, D., Amorim, A., Bianchi, F., Breitenlechner, M., David, A., Dommen, J., Downard, A., Ehn, M., Flagan, R. C., Haider, S., Hansel, A., Hauser, D., Jud, W., Junninen, H., Kreissl, F., Kvashin, A., Laaksonen, A., Lehtipalo, K., Lima, J., Lovejoy, E. R., Makhmutov, V., Mathot, S., Mikkilä, J., Minginette, P., Mogo, S., Nieminen, T., Onnela, A., Pereira, P., Petäjä, T., Schnitzhofer, R., Seinfeld, J. H., Sipilä, M., Stozhkov, Y., Stratmann, F., Tomé, A., Vanhanen, J., Viisanen, Y., Vrtala, A., Wagner, P. E., Walther, H., Weingartner, E., Wex, H., Winkler, P. M., Carslaw, K. S., Worsnop, D. R., Baltensperger, U., and Kulmala, M.: Role of sulphuric acid, ammonia and galactic cosmic rays in atmospheric aerosol nucleation, Nature, 476, 429–433, https://doi.org/10.1038/nature10343, 2011.

Knowlton, N., Brainard, R. E., Fisher, R., Moews, M., Plaisance, L., and Caley, M. J.: Coral Reef Biodiversity, in: Life in the World's Oceans, John Wiley & Sons, Ltd, 65–78, https://doi.org/10.1002/9781444325508.ch4, 2010.

Kulmala, M., Maso, M. D., Mäkelä, J. M., Pirjola, L., Väkevä, M., Aalto, P., Miikkulainen, P., Hämeri, K., and O'dowd, C. D.: On the formation, growth and composition of nucleation mode particles, Tellus B Chem. Phys. Meteorol., 53, 479–490, https://doi.org/10.3402/tellusb.v53i4.16622, 2001.

Kulmala, M., Laakso, L., Lehtinen, K. E. J., Riipinen, I., Dal Maso, M., Anttila, T., Kerminen, V.-M., Hõrrak, U., Vana, M., and Tammet, H.: Initial steps of aerosol growth, Atmos. Chem. Phys., 4, 2553–2560, https://doi.org/10.5194/acp-4-2553-2004, 2004.

Lehtipalo, K., Nieminen, T., Schobesberger, S., Ehn, M., Kulmala, M., and Kerminen, V.-M.: How the understanding of atmospheric new particle formation has evolved along with the development of measurement and analysis methods, J. Aerosol Sci., 184, 106494, https://doi.org/10.1016/j.jaerosci.2024.106494, 2025.

Li, Z., Harrison, L., Alroe, J., Scoble, H., Chen, C., Medcraft, C., Holloway, C., Brown, R., Baker, P., Harrison, D. P., and Ristovski, Z.: Characterizing the Crosswind Structure of Artificial Seawater Droplet Plumes during a Sea Trial on the Great Barrier Reef, Environ. Sci. Technol., 59, 27222–27229, https://doi.org/10.1021/acs.est.5c10024, 2025.

https://doi.org/10.5194/egusphere-2026-4869
Preprint. Discussion started: 21 August 2026

McFiggans, G., Artaxo, P., Baltensperger, U., Coe, H., Facchini, M. C., Feingold, G., Fuzzi, S., Gysel, M., Laaksonen, A., Lohmann, U., Mentel, T. F., Murphy, D. M., O'Dowd, C. D., Snider, J. R., and Weingartner, E.: The effect of physical and chemical aerosol properties on warm cloud droplet activation, Atmos. Chem. Phys., 6, 2593–2649, https://doi.org/10.5194/acp-6-2593-2006, 2006.

Modini, R. L., Ristovski, Z. D., Johnson, G. R., He, C., Surawski, N., Morawska, L., Suni, T., and Kulmala, M.: New particle formation and growth at a remote, sub-tropical coastal location, Atmos. Chem. Phys., 9, 7607–7621, https://doi.org/10.5194/acp-9-7607-2009, 2009.

Ng, N. L., Canagaratna, M. R., Zhang, Q., Jimenez, J. L., Tian, J., Ulbrich, I. M., Kroll, J. H., Docherty, K. S., Chhabra, P. S., Bahreini, R., Murphy, S. M., Seinfeld, J. H., Hildebrandt, L., Donahue, N. M., DeCarlo, P. F., Lanz, V. A., Prévôt, A. S. H., Dinar, E., Rudich, Y., and Worsnop, D. R.: Organic aerosol components observed in Northern Hemispheric datasets from Aerosol Mass Spectrometry, Atmos. Chem. Phys., 10, 4625–4641, https://doi.org/10.5194/acp-10-4625-2010, 2010.

Nieminen, T., Kerminen, V.-M., Petäjä, T., Aalto, P. P., Arshinov, M., Asmi, E., Baltensperger, U., Beddows, D. C. S., Beukes, J. P., Collins, D., Ding, A., Harrison, R. M., Henzing, B., Hooda, R., Hu, M., Hõrrak, U., Kivekäs, N., Komsaare, K., Krejci, R., Kristensson, A., Laakso, L., Laaksonen, A., Leaitch, W. R., Lihavainen, H., Mihalopoulos, N., Németh, Z., Nie, W., O'Dowd, C., Salma, I., Sellegri, K., Svenningsson, B., Swietlicki, E., Tunved, P., Ulevicius, V., Vakkari, V., Vana, M., Wiedensohler, A., Wu, Z., Virtanen, A., and Kulmala, M.: Global analysis of continental boundary layer new particle formation based on long-term measurements, Atmos. Chem. Phys., 18, 14737–14756, https://doi.org/10.5194/acp-18-14737-2018, 2018.

Noble, S. R. and Hudson, J. G.: Effects of Continental Clouds on Surface Aitken and Accumulation Modes, J. Geophys. Res. Atmos., 124, 5479–5502, https://doi.org/10.1029/2019JD030297, 2019.

O'Dowd, C. D., Jimenez, J. L., Bahreini, R., Flagan, R. C., Seinfeld, J. H., Hämeri, K., Pirjola, L., Kulmala, M., Jennings, S. G., and Hoffmann, T.: Marine aerosol formation from biogenic iodine emissions, Nature, 417, 632–636, https://doi.org/10.1038/nature00775, 2002.

Peltola, M., Rose, C., Trueblood, J. V., Gray, S., Harvey, M., and Sellegri, K.: New particle formation in coastal New Zealand with a focus on open-ocean air masses, Atmos. Chem. Phys., 22, 6231–6254, https://doi.org/10.5194/acp-22-6231-2022, 2022.

Petters, M. D. and Kreidenweis, S. M.: A single parameter representation of hygroscopic growth and cloud condensation nucleus activity, Atmos. Chem. Phys., 7, 1961–1971, https://doi.org/10.5194/acp-7-1961-2007, 2007.

https://doi.org/10.5194/egusphere-2026-4869
Preprint. Discussion started: 21 August 2026

Quinn, P. K. and Bates, T. S.: The case against climate regulation via oceanic phytoplankton sulphur emissions, Nature, 480, 51–56, https://doi.org/10.1038/nature10580, 2011.

Reaka, M.: The global biodiversity of coral reefs: a comparison with rainforests, 1997.

Rowland, M. J., Lambrides ,Ariana B. J., McNiven ,Ian J., and and Ulm, S.: Great Barrier Reef Indigenous archaeology and occupation of associated reef and continental islands, Australas. J. Environ. Manag., 32, 22–45, https://doi.org/10.1080/14486563.2024.2336969, 2025.

Santavy, D. L., Horstmann, C. L., Sharpe, L. M., Yee, S. H., and Ringold, P.: What is it about coral reefs? Translation of ecosystem goods and services relevant to people and their well-being, Ecosphere Wash. DC, 12, 1–27, https://doi.org/10.1002/ecs2.3639, 2021.

Shaw, S. L., Gantt, B., and Meskhidze, N.: Production and Emissions of Marine Isoprene and Monoterpenes: A Review, Adv. Meteorol., 2010, 408696, https://doi.org/10.1155/2010/408696, 2010.

Sihto, S.-L., Mikkilä, J., Vanhanen, J., Ehn, M., Liao, L., Lehtipalo, K., Aalto, P. P., Duplissy, J., Petäjä, T., Kerminen, V.-M., Boy, M., and Kulmala, M.: Seasonal variation of CCN concentrations and aerosol activation properties in boreal forest, Atmos. Chem. Phys., 11, 13269–13285, https://doi.org/10.5194/acp-11-13269-2011, 2011.

Sipilä, M., Sarnela, N., Jokinen, T., Henschel, H., Junninen, H., Kontkanen, J., Richters, S., Kangasluoma, J., Franchin, A., Peräkylä, O., Rissanen, M. P., Ehn, M., Vehkamäki, H., Kurten, T., Berndt, T., Petäjä, T., Worsnop, D., Ceburnis, D., Kerminen, V.-M., Kulmala, M., and O'Dowd, C.: Molecular-scale evidence of aerosol particle formation via sequential addition of HIO3, Nature, 537, 532–534, https://doi.org/10.1038/nature19314, 2016.

Stefels, J., Steinke, M., Turner, S., Malin, G., and Belviso, S.: Environmental constraints on the production and removal of the climatically active gas dimethylsulphide (DMS) and implications for ecosystem modelling, Biogeochemistry, 83, 245–275, https://doi.org/10.1007/s10533-007-9091-5, 2007.

Stein, A. F., Draxler, R. R., Rolph, G. D., Stunder, B. J. B., Cohen, M. D., and Ngan, F.: NOAA's HYSPLIT Atmospheric Transport and Dispersion Modeling System, Bull. Am. Meteorol. Soc., 96, 2059–2077, https://doi.org/10.1175/BAMS-D-14-00110.1, 2015.

Storelvmo, T., Leirvik, T., Lohmann, U., Phillips, P. C. B., and Wild, M.: Disentangling greenhouse warming and aerosol cooling to reveal Earth's climate sensitivity, Nat. Geosci., 9, 286–289, https://doi.org/10.1038/ngeo2670, 2016.

Sulo, J., Okuljar, M., Alroe, J., Li, Z., Horchler, E. J., Cravigan, L., Miljevic, B., Harrison, L., Harrison, D., and Ristovski, Z.: Coral reef exposure increases aerosol and cloud

https://doi.org/10.5194/egusphere-2026-4869
Preprint. Discussion started: 21 August 2026

condensation nuclei over the Great Barrier Reef, Aerosol Res. Discuss., 1–22, https://doi.org/10.5194/ar-2026-9, 2026a.

Sulo, J., Okuljar, M., Alroe, J., Li, Z., Horchler, E. J., Cravigan, L., Miljevic, B., Harrison, L., Harrison, D., and Ristovski, Z.: Coral reef exposure increases aerosol and cloud condensation nuclei over the Great Barrier Reef, Aerosol Res. Discuss., 1–22, https://doi.org/10.5194/ar-2026-9, 2026b.

Swan, H. B.: The Potential for Great Barrier Reef Regional Climate Regulation via Dimethylsulfide Atmospheric Oxidation Products, Front. Mar. Sci., 9, https://doi.org/10.3389/fmars.2022.869166, 2022.

Swan, H. B., Crough, R. W., Vaattovaara, P., Jones, G. B., Deschaseaux, E. S. M., Eyre, B. D., Miljevic, B., and Ristovski, Z. D.: Dimethyl sulfide and other biogenic volatile organic compound emissions from branching coral and reef seawater: potential sources of secondary aerosol over the Great Barrier Reef, J. Atmos. Chem., 73, 303–328, https://doi.org/10.1007/s10874-016-9327-7, 2016.

Twomey, S.: Pollution and the planetary albedo, Atmos. Environ. 1967, 8, 1251–1256, https://doi.org/10.1016/0004-6981(74)90004-3, 1974.

Wang, X., Jacob, D. J., Downs, W., Zhai, S., Zhu, L., Shah, V., Holmes, C. D., Sherwen, T., Alexander, B., Evans, M. J., Eastham, S. D., Neuman, J. A., Veres, P. R., Koenig, T. K., Volkamer, R., Huey, L. G., Bannan, T. J., Percival, C. J., Lee, B. H., and Thornton, J. A.: Global tropospheric halogen (Cl, Br, I) chemistry and its impact on oxidants, Atmos. Chem. Phys., 21, 13973–13996, https://doi.org/10.5194/acp-21-13973-2021, 2021.

Wildt, J., Mentel, T. F., Kiendler-Scharr, A., Hoffmann, T., Andres, S., Ehn, M., Kleist, E., Müsgen, P., Rohrer, F., Rudich, Y., Springer, M., Tillmann, R., and Wahner, A.: Suppression of new particle formation from monoterpene oxidation by NO_x, Atmos. Chem. Phys., 14, 2789–2804, https://doi.org/10.5194/acp-14-2789-2014, 2014.

Yassaa, N., Peeken, I., Zöllner, E., Bluhm, K., Arnold, S., Spracklen, D., and Williams, J.: Evidence for marine production of monoterpenes, Environ. Chem., 5, 391–401, https://doi.org/10.1071/EN08047, 2008.

Zhao, D., Schmitt, S. H., Wang, M., Acir, I.-H., Tillmann, R., Tan, Z., Novelli, A., Fuchs, H., Pullinen, I., Wegener, R., Rohrer, F., Wildt, J., Kiendler-Scharr, A., Wahner, A., and Mentel, T. F.: Effects of NO_x and SO_2 on the secondary organic aerosol formation from photooxidation of α-pinene and limonene, Atmos. Chem. Phys., 18, 1611–1628, https://doi.org/10.5194/acp-18-1611-2018, 2018.

Zheng, G., Wang, Y., Wood, R., Jensen, M. P., Kuang, C., McCoy, I. L., Matthews, A., Mei, F., Tomlinson, J. M., Shilling, J. E., Zawadowicz, M. A., Crosbie, E., Moore, R., Ziemba, L.,

https://doi.org/10.5194/egusphere-2026-4869
Preprint. Discussion started: 21 August 2026

860 Andreae, M. O., and Wang, J.: New particle formation in the remote marine boundary layer, Nat. Commun., 12, 527, https://doi.org/10.1038/s41467-020-20773-1, 2021.